Effects of Nd- and Zr- substitution for Sm on magnetic and structural properties in $SmFe_{11}V$ 1:12 compound

A.M. Schönhöbel, R. Madugundo, C. Echevarria-Bonet, L.E. Zamora, J.M. Barandiarán, G.C. Hadjipanayis

PII: S0925-8388(23)00570-4

DOI: https://doi.org/10.1016/j.jallcom.2023.169267

Reference: JALCOM169267

To appear in: *Journal of Alloys and Compounds*

Received date: 14 September 2022
Revised date: 3 February 2023
Accepted date: 11 February 2023

Please cite this article as: A.M. Schönhöbel, R. Madugundo, C. Echevarria-Bonet, L.E. Zamora, J.M. Barandiarán and G.C. Hadjipanayis, Effects of Nd- and Zr- substitution for Sm on magnetic and structural properties in $SmFe_{11}V$ 1:12 compound, *Journal of Alloys and Compounds,* (2022) doi:https://doi.org/10.1016/j.jallcom.2023.169267

Effects of Nd- and Zr- substitution for Sm on magnetic and structural properties in $SmFe_{11}V$ 1:12 compound

A. M. Schönhöbel[a,b], R. Madugundo[b], C. Echevarria-Bonet[b,d], L. E. Zamora[a], J. M. Barandiarán[c], G. C. Hadjipanayis[e]

[a]*Centro de Excelencia en Nuevos Materiales (CENM), Universidad del Valle, 25360 Cali, Colombia*
[b]*BCMaterials, UPV/EHU Science Park, 48940 Leioa, Spain*
[c]*Department of Electricity and Electronics, University Basque Country (UPV/EHU), 48940 Leioa, Spain*
[d]*Department of Physics, University of Oviedo, 33007 Oviedo, Spain*
[e]*Department of Physics and Astronomy, University of Delaware, Newark, DE, 19716, USA*

Abstract

Structural and magnetic properties of polycrystalline alloys of $Sm_{1-x}Y_xFe_{11}V$ [Y=Nd ($0 \le x \le 0.4$), Zr ($0 \le x \le 0.6$)] were investigated. Substitution of Nd for Sm promoted the formation of α-(Fe,V) and 3:29 phases. In the case of Zr-substitution, all the optimally heat-treated alloys crystallize into tetragonal $ThMn_{12}$-type structure 1:12 phase and bcc α-(Fe,V) phase. For high Zr content of $x = 0.4$ and 0.6, Laves phase $ZrFe_2$ was also detected with Curie temperature of 709 and 697 K, respectively. The substitution of Zr resulted in a contraction of 0.7% of the 1:12 cell volume. Oriented powder XRD patterns indicated that the easy magnetization direction was along (002) *c*-axis. As Zr content increased from $x = 0$ to 0.6, anisotropy field decreased from 11 to 9 T and Curie temperature from 625 to 583 K. On the other hand, the saturation magnetization increased from 114 to 138 $Am^2\,kg^{-1}$. Among the alloys investigated in the present study, the $Sm_{0.61}Zr_{0.40}Fe_{11.03}V_{0.96}$ with saturation magnetization of 129 $Am^2\,kg^{-1}$, anisotropy field of 9.4 T and Curie temperature of 599 K is the most favorable candidate for permanent magnet applications.

Keywords: Hard magnets, $ThMn_{12}$-type structure, iron alloys, rare-earth lean magnets.

1. Introduction

In response to the increasing limitations on critical rare-earth (R) metals supplies [1, 2], a global effort is being devoted to find R-lean/free magnetic phases suitable for permanent magnet applications [3]. As a result, there has been a renewed interest in $R(Fe,M)_{12}$ (M is transition metal, such as Ti, V, Mo, Si, used as stabilizer of the 1:12 phase) compounds because of their reduced R concentration (7.7 at.% as compared with 11.8 at.% in $Nd_2Fe_{14}B$, 16.7 at.% in $SmCo_5$ and 10.5 at.% in Sm_2Co_{17}), excellent intrinsic magnetic properties and a simple crystal structure. The structure is tetragonal $ThMn_{12}$-type, I4/mmm space group, with three nonequivalent sites (8*i*, 8*j* and 8*f*) for Fe and M together and one site (2*a*) for R [4]. The most promising candidate materials are those with R = Nd and Sm. Figure 1 shows Curie temperature (T_C), saturation magnetization ($\mu_0 M_s$) and magnetocrystalline anisotropy ($\mu_0 H_A$) of the most investigated 1:12 compounds [5–21].

Previous studies have shown that the $SmFe_{12}$-based compounds as potential candidates for permanent magnet applications as it has been possible to get coercivities up to 1.1 T [22–28] in Sm-Fe-V alloy (bulk and ribbons), and 1.32 T [29] in $Sm(Fe_{0.8}Co_{0.2})_{12}$ alloy (thin films). However, for bulk alloys, the remanence observed has been relatively low (< 0.5 T). It is necessary to increase the remanence via texture or increasing saturation magnetization along with the stability of 1:12 phase. In this direction, there had been investigations where Sm was partially or fully substituted by other R elements or non R elements such as Zr. Substitution of Sm by Ce, Pr, Gd, Tb or Dy in $SmFe_{11}Ti$ resulted in decreasing $\mu_0 H_A$ and $\mu_0 M_s$ [27, 30, 31]. More recently Zhao et al. [32] studied the core–shell structure (Sm-rich shell and Y-rich core) in $(Sm_{0.75}Y_{0.25})Fe_{0.8}Co_{0.2})_{11.25}Ti_{0.75}$ alloy, as Y substitution not only can stabilize the $ThMn_{12}$-type structure, but also suppress the precipitation of the α-Fe phase. On the other hand, when Sm is substituted by Nd the $\mu_0 M_s$ either remained unchanged [31] or increased [33]. Kim et al. [31] reported that $\mu_0 H_A$ decreased more than 75% when half of Sm was substituted by Nd in $SmFe_{11}Ti$, while Niarchos et al. [33] reported a decrease of 50%.

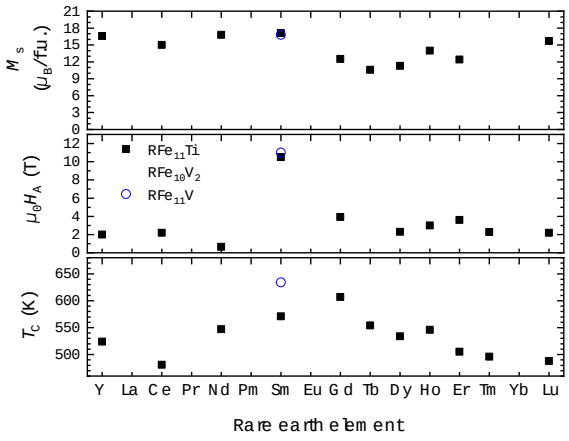

Figure 1: Intrinsic magnetic properties of $R(Fe,Ti)_{12}$ and $R(Fe,V)_{12}$ for different R elements [5–21].

Tozman et al. [34] investigated the effect of V on the phase stability and intrinsic magnetic properties of $SmFe_{12-x}V_x$ ($0 \leq x \leq 1.9$) thin films demonstrating V-substituted compounds with 7 at.% phase stabilizers have more merit than Ti-substituted ones.

The last decade there have been reports investigating the stability of the $R(Fe,M)_{12}$ phase by replacing the R (R = Nd or Sm) with less expensive R metals such as Ce [35, 36] or by non R metals such as Zr [37–39]. Among them, R-Fe-Ti and R-Fe-Si systems have been widely investigated. According to the previous studies [40, 41], Zr atoms occupy only the rare-earth 2*a* sites. Sakurada et al. [42] reported that substitution of Nd with Zr stabilized the 1:12 phase up to $x \approx 0.75$ in $Nd_{1-x}Zr_xFe_{10}Si_2$. More recently Gabay et al. [43] synthesized $Zr(Fe,Si)_{12}$, the first R-free 1:12 compound. They reported a $ZrFe_{10.4}Si_{1.6}$ alloy with $\mu_0 M_s$ of 1.15 T but with a very weak $\mu_0 H_A \approx 1.9$ T. Partial substitution of Zr with R = Y, La, Ce, Pr and Sm has been investigated by Gabay et al. [44]. In terms of $\mu_0 H_A$, the effect of Sm was the strongest with a value of 4.07 T in $Zr_{0.7}Sm_{0.3}Fe_{10}Si_2$. In the same direction, Tozman et al. [39] attained the 1:12 phase in $Sm_{1-y}Zr_y(Fe_{0.8}Co_{0.2})_{11.5}Ti_{0.5}$ alloys with small concentration of Zr (y = 0.1 to 0.3). However, with increase in Zr content from y = 0.1 to 0.3, $\mu_0 M_s$ decreased from 1.61 to 1.52 T and $\mu_0 H_A$ from 9.2 to 7.9 T. A maximum T_C of 830 K was reported for $Sm_{0.8}Zr_{0.2}(Fe_{0.8}Co_{0.2})_{11.5}Ti_{0.5}$ alloy.

Up to now, no study has been reported on the intrinsic magnetic properties of $(Sm,R)Fe_{11}V$ compounds. This paper studies the effect on the structural, microstructural, thermal and magnetic properties of the Sm-substitution by Nd in $Sm_{1-x}Nd_xFe_{11}V$ ($0 \leq x \leq 0.4$) and by Zr in $Sm_{1-x}Zr_xFe_{11}V$ ($0 \leq x \leq 0.6$) alloys. The $SmFe_{11}V$ alloy was chosen as it has a strong $\mu_0 H_A$, a relatively high $\mu_0 M_s$ and T_C, which are suitable for permanent magnet applications [20].

2. Experiment

Polycrystalline samples were prepared by arc melting the constituent elements under argon atmosphere in a water-cooled copper crucible. The ingots were turned over and remelted three times to ensure their homogeneity. The Sm losses were compensated by adding an appropriate excess of Sm. The as-cast ingots were sealed in evacuated quartz tubes filled with Ar, heat-treated at temperatures ranging from 1000 to 1100°C for 3-4 days and quenched in water.

X-ray diffraction (XRD) and room-temperature magnetic measurements were performed on powders prepared by hand grinding. The XRD patterns were taken using a Rigaku Ultima IV diffractometer with Cu-K_α (λ = 1.5418 Å) radiation in backscattering Bragg-Brentano geometry. For structural characterization, analysis of the XRD patterns was performed using a FullProf suite [45] based on the Rietveld method [46]. Easy-axis magnetization was found from the intensities of lines on diffractograms of magnetically oriented powder samples.

Magnetization was measured with a VersaLab 3 T cryogen-free PPMS from Quantum Design and a high field VSM with a superconducting magnet (up to 14 T) cooled with He closed circuit refrigerator (CFMS from Cryogenic Ltd). The $\mu_0 H_A$ estimation was performed on oriented samples which were prepared by mixing the powders (< 44 µm) with a cold-curing epoxy and dried under a 2 T magnetic field. The demagnetization factor of the aligned powders was considered negligible as the $\mu_0 H_A$ was large enough. The T_C was obtained from $M(T)$ measurements at an applied field of 0.05 T for small (≈ 15 mg) heat-treated samples.

Microscopic analysis of polished unetched alloy samples was carried out by using Hitachi TM3000 Tabletop scanning electron microscope (SEM) and the composition analysis was performed with a Quantax70 energy dispersive X-ray spectroscopy (EDX) detector.

3. Results and Discussion

Figure 2 presents XRD patterns of $Sm_{1-x}Nd_xFe_{11}V$ (x = 0, 0.2 and 0.4) alloys heat-treated at 1100°C for 4 days.

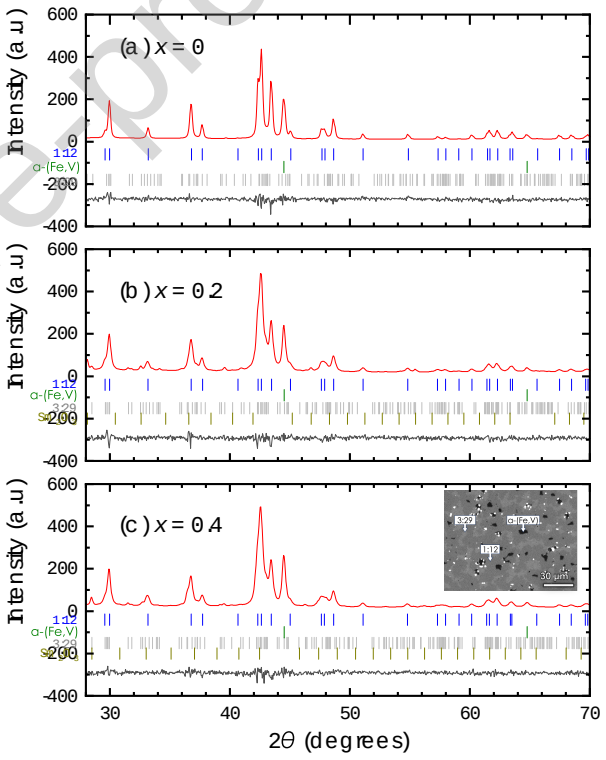

Figure 2: Experimental (black dots) and calculated (continuous line) XRD patterns of $Sm_{1-x}Nd_xFe_{11}V$ alloys heat-treated at 1100°C for 4 days (a) x = 0, (b) x = 0.2 and (c) x = 0.4. Boxes include the error and small vertical lines refer to Bragg peak positions of the phases present. Inset in Fig. 2(c) corresponds to the BSE-SEM micrograph of x = 0.4 alloy.

The diffraction patterns of all the samples present characteristic lines corresponding to the 1:12, 3:29 and α-(Fe,V) phases. For the case of x = 0.2 and 0.4 small amount of Sm_2O_3 is also observed. Although the 1:12 phase is maintained throughout the Nd-substitution, Nd promotes the formation of the 3:29 phase (Nd_3Fe_{29})-type structure with the monoclinic symmetry and C2/m space group). Observation of the 3:29 phase is consistent with the existing ternary equilibria of Sm-Fe-V at 1100 and 1200°C (both for 20 h) [47]. From the phase diagram

(1100°C) in the reference, we can see that there are two phase fields near pure 1:12 phase, 3:29+α-(Fe,V) and 1:12 +α-(Fe,V). Considering our slightly different annealing conditions (longer durations), formation of 3:29 phase along with 1:12 is possible in $Sm_{7.7}Fe_{84.6}V_{7.7}$ and in $(Sm,Nd)_{7.7}Fe_{84.6}V_{7.7}$.

Volume fractions and lattice parameters of each phase derived from the Rietveld analysis are listed in Table 1. The SEM-EDX composition analysis confirmed the results obtained by XRD. For $x = 0.4$ sample (inset in Fig. 2c) the matrix in dark gray corresponds to the 1:12 phase, this exists together with α-(Fe,V) in black, and a minor phase in light gray which is identified as 3:29. The small bright spots correspond to free Sm. This phase was not observed in the XRD due to its low volume fraction. The chemical composition of the 1:12 phase obtained by SEM-EDX analysis are listed in table 2.

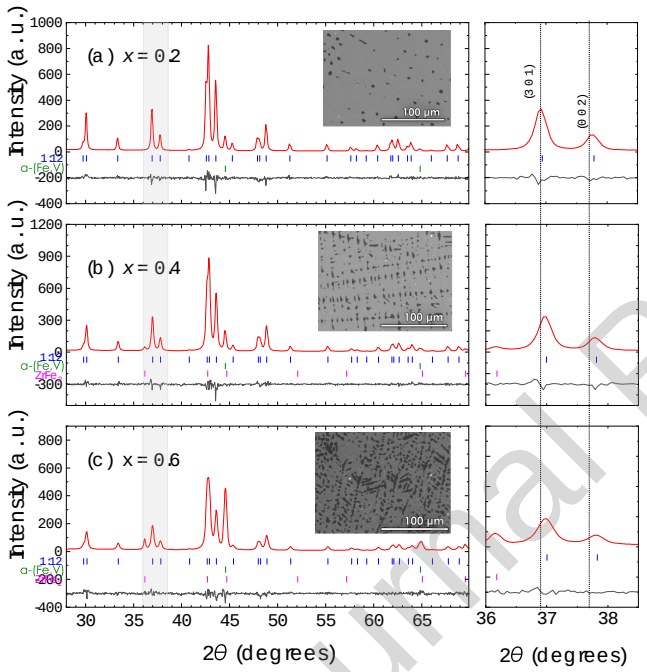

Figure 3: Experimental (black dots) and calculated (continuous line) XRD patterns of optimally heat-treated $Sm_{1-x}Zr_xFe_{11}V$ alloys (a) $x = 0.2$ (b) $x = 0.4$ and (d) $x = 0.6$. Small vertical lines refer to Bragg peak positions of phases present and the error is shown below them. Enlarged peaks from the gray regions are shown at the right side. Insets correspond to the SEM-BSE images of the respective samples.

Figure 3 displays the XRD patterns of the optimally heat-treated $Sm_{1-x}Zr_xFe_{11}V$ ($x = 0.2, 0.4$ and 0.6) alloys. The major phase in all these samples is 1:12, followed by α-(Fe,V) and the cubic Laves phase $ZrFe_2$ ($MgCu_2$-type, $Fd\bar{3}m$ space group). As Zr content increases, the α-(Fe,V) phase increases and the Laves phase precipitates for $x \geq 0.4$. This is in agreement with the frequent formation of Laves phase compounds in alloys involving transition metals [48]. Volume fractions and lattice parameters of each phase present derived from the Rietveld analysis are listed in Table 1. As Zr has a smaller atomic radius (1.60 Å [49]) than Sm (1.80 Å [49]), the increase in Zr results in lattice contraction as observed from the 1:12 peaks shifting towards higher 2θ angles as shown in Fig. 3 enlarged (301) and (002) peaks at the right side.

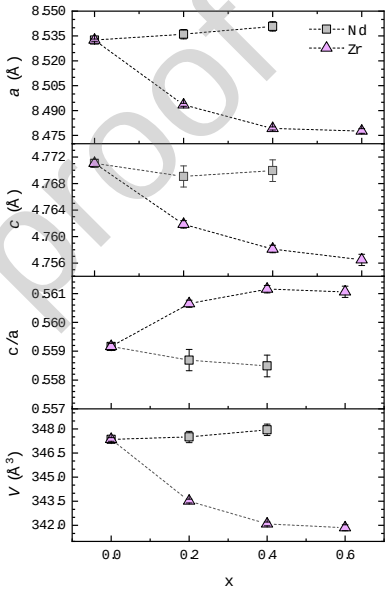

Figure 4: Lattice parameters (a and c), c/a ratio and unit cell volume (V) of the 1:12 phase of heat-treated $Sm_{1-x}Nd_xFe_{11}V$ and $Sm_{1-x}Zr_xFe_{11}V$ alloys.

Lattice parameters a and c, c/a ratio and cell volume (V) of the 1:12 phase for Zr- and Nd-substitution are shown in Fig. 4. The parameter a decreases from 8.532 to 8.478 Å and c from 4.771 to 4.756 Å with increasing Zr from $x = 0$ to 0.6. An increase in c/a ratio can also be seen. The unit cell contraction comes with a 0.7% of volume reduction. Tozman et al. [39] reported a contraction of lattice parameter a from 8.53 to 8.50 Å in $Sm_{1-y}Zr_y(Fe_{0.8}Co_{0.2})_{11.5}Ti_{0.5}$ alloys with increasing y from 0 to 0.3. In contrast, expansion of the lattice with increasing Nd content occurs predominantly in the basal plane, resulting in a decrease of c/a ratio. The expansion comes with a 0.2%

Table 1: Volume fractions and lattice parameters of the phases present in $Sm_{1-x}Nd_xFe_{11}V$ and $Sm_{1-x}Zr_xFe_{11}V$ heat-treated alloys.

		Volume fraction					Lattice parameters								
							1:12		α-(Fe,V)	3:29				Sm_2O_3	$ZrFe_2$
x	composition	1:12	α-(Fe,V)	3:29	Sm_2O_3	$ZrFe_2$	a(Å)	c(Å)	a(Å)	a(Å)	b(Å)	c(Å)	β	a(Å)	a(Å)
0.0	$Sm_{0.95}Fe_{10.97}V_{1.08}$	0.796	0.152	0.052			8.532	4.771	2.879	10.568	8.523	9.709	96.855		
0.2	$Sm_{0.80}Nd_{0.20}Fe_{11.00}V_{1.00}$	0.695	0.135	0.156	0.014		8.536	4.769	2.878	10.612	8.546	9.720	96.877	10.986	
0.4	$Sm_{0.59}Nd_{0.40}Fe_{10.99}V_{1.02}$	0.667	0.146	0.176	0.011		8.541	4.770	2.878	10.629	8.561	9.710	96.817	10.851	
0.2	$Sm_{0.77}Zr_{0.20}Fe_{10.98}V_{1.05}$	0.95	0.05				8.494	4.762	2.876						
0.4	$Sm_{0.61}Zr_{0.40}Fe_{11.03}V_{0.96}$	0.91	0.06			0.03	8.479	4.758	2.877						7.021
0.6	$Sm_{0.40}Zr_{0.60}Fe_{11.02}V_{0.98}$	0.70	0.23			0.07	8.478	4.756	2.875						7.022

of volume increment from $x = 0$ to 0.4. In the case of Nd-substitution in $SmFe_{11}Ti$ reported by Niarchos et al. [33], there is an increase of a from 8.5572 to 8.5639 Å and a decrease of c/a ratio from 0.5609 to 0.5592 with increasing Nd from $x = 0$ to 0.5.

Insets in Fig 3(a), (b) and (c) show SEM-BSE micrographs of the heat-treated alloys $x = 0.2$, 0.4 and 0.6 respectively. Narrow dendrites of α-(Fe,V) phase between 5 and 20 µm are formed and uniformly distributed, the matrix phase is identified as 1:12 phase, and the light gray areas as the $ZrFe_2$ Laves phase, the latter is only visible for $x = 0.6$. A SEM-BSE micrograph and EDX elemental mappings for $x = 0.6$ are shown in Fig. 5. Segregation of α-(Fe,V) and $ZrFe_2$ phases can be seen where, the former are represented by the green-red dendrites and the latter by the blue-greens. The chemical composition of the 1:12 phase determined by SEM-EDX are listed in Table 2.

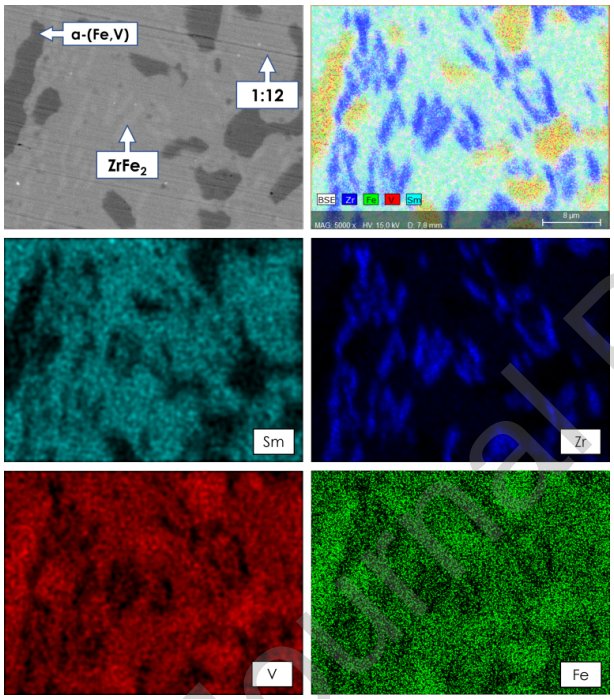

Figure 5: SEM-BSE micrographs and EDX composition maps of Sm, Zr, V and Fe elements from the polished surface of the optimally heat-treated $Sm_{0.4}Zr_{0.6}Fe_{11}V$ alloy.

Table 2: Intrinsic magnetic properties of 1:12 phase in $Sm_{1-x}Y_xFe_{11}V$ (Y=Nd, Zr) alloys and their composition determined by SEM-EDX. Magnetization values given in parenthesis are in T.

x	Composition	M_s ($Am^2\,kg^{-1}$)	$\mu_0 H_A$ (T)	T_C (K)
0.0	$Sm_{0.95}Fe_{10.97}V_{1.08}$	114 (1.11)	11.0	625
0.2	$Sm_{0.80}Nd_{0.20}Fe_{11.00}V_{1.00}$	111 (1.08)	10.6	608
0.4	$Sm_{0.59}Nd_{0.40}Fe_{10.99}V_{1.02}$	109 (1.06)	7.4	593
0.2	$Sm_{0.77}Zr_{0.20}Fe_{10.98}V_{1.05}$	115 (1.13)	10.2	608
0.4	$Sm_{0.61}Zr_{0.40}Fe_{11.03}V_{0.96}$	129 (1.28)	9.4	599
0.6	$Sm_{0.40}Zr_{0.60}Fe_{11.02}V_{0.98}$	138 (1.37)	9.0	583

Figure 6 (left) shows room-temperature initial magnetization curves of the oriented powders of $Sm_{1-x}Y_xFe_{11}V$ (Y=Nd, Zr) alloys measured ∥ and ⊥ to the magnetic field orientation direction. On the right side, corresponding XRD patterns of the oriented powders are shown. The M_s values for the 1:12 phase were deduced by subtracting the contribution from the secondary phases (magnetization at room temperature: $M_{3:29}$=78.8 $Am^2\,kg^{-1}$ [50], $M_{\alpha\text{-Fe}}$=218 $Am^2\,kg^{-1}$ [51] and M_{ZrFe_2}=43.2 $Am^2\,kg^{-1}$ [52]) taking into account their volume fractions from the XRD analysis (Table 1). In the case of Zr-substitution, M_s at room temperature increases from 114 to 138 $Am^2\,kg^{-1}$ (1.11 to 1.37 T) with increasing Zr from $x = 0$ to 0.6. Kuno et al. [53] reported an increase in $\mu_0 M_s$ of 1:12 phase from 1.50 to 1.58 T with increase in Zr from $y = 0$ to 0.2 in $Sm_{1-y}Zr_y(Fe_{0.8}Co_{0.2})_{11.5}Ti_{0.5}$ alloys. Also Tozman et al. [54] reported an increase in $\mu_0 M_s$ from 1.78 to 1.90 T with increasing Zr-substitution from x = 0 to 0.26 in $Sm_{1-x}Zr_x(Fe_{0.8}Co_{0.2})_{12}$ thin films. The enhancement in $\mu_0 M_s$ was recently explained (by using XAFS technique) as a result of electron transfer from Zr to the Fe 8*f* atoms which causes an increase in the magnetic moment and magnetic interactions in the Fe 8*f* site [55]. For Nd-substitution, M_s at room temperature decreases from 114 $Am^2\,kg^{-1}$ (1.11 T) in $x = 0$ to 109 $Am^2\,kg^{-1}$ (1.06 T) in $x = 0.4$. A similar behavior was reported by Kim et al. [31] when half of Sm was substituted for Nd in $SmFe_{11}Ti$ alloy, the $\mu_0 M_s$ decreased from 1.27 to 1.21 T.

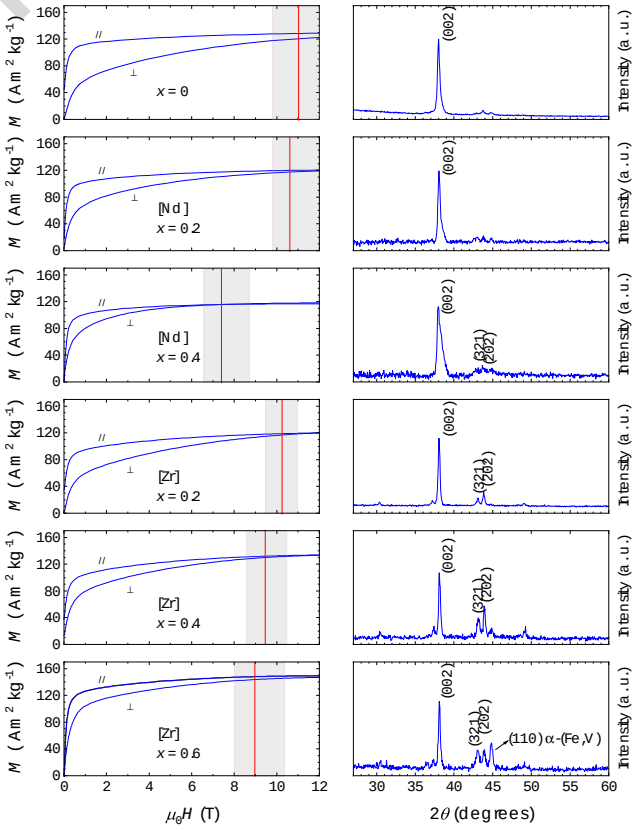

Figure 6: (Left) Magnetization at room temperature measured ∥ and ⊥ to the orientation direction as a function of applied field for optimally heat-treated $Sm_{1-x}Nd_xFe_{11}V$ and $Sm_{1-x}Zr_xFe_{11}V$ alloys. (Right) Corresponding XRD data of oriented optimally heat-treated samples.

The $\mu_0 H_A$ was determined by plotting M in the perpendicular direction as a function of $[(\mu_0 H)^{-2}]$ [56] from Fig. 6, and it was obtained from the minimum of the derivative [20, 39, 57]. The highlighted region in the plots shows the uncertainty in determining the anisotropy field (see supplementary data). Table 2 summarizes the intrinsic magnetic properties. As Zr content is increased, $\mu_0 H_A$ decreases from 11 T ($x = 0$) to 9 T ($x = 0.6$). Even for highest Zr content the $\mu_0 H_A$ is still higher than NdFeB anisotropy field (6.7 T [58]). Tozman et al. [39, 54] reported a decrease in $\mu_0 H_A$ on substitution of Zr for Sm in $Sm_{1-y}Zr_y(Fe_{0.8}Co_{0.2})_{11.5}Ti_{0.5}$ bulk alloys and in $Sm_{1-x}Zr_x(Fe_{0.8}Co_{0.2})_{12}$ thin films. This decrease in $\mu_0 H_A$ with increasing Zr is attributed to the decrease of R content. The high anisotropy is mainly due to the R element, this property is linked to the magnetic coupling between the R and M sublattices [59]. In accordance with the anisotropy field, XRD measurements of field oriented powder samples indicate that the easy-axis of magnetization is along the c-axis (002). The other reflexions such as (321) and (202) are attributed to the presence of the secondary phases or misoriented grains. In case of Nd-substitution, $\mu_0 H_A$ decreases from 11 to 7.4 T with increasing Nd from $x = 0$ to 0.4, respectively. Kim et al. [31] and Niarchos et al. [33] reported a similar decrease in $\mu_0 H_A$ on Nd-substitution in $SmFe_{11}Ti$ alloy system.

All the magnetization curves measured in direction $\perp$ to the orientation have a curvature in the low-field region. This can be due to the combination of two effects, the presence of a soft phase of high susceptibility α-(Fe,V), and poor alignment, as the particles (size < 44 µm) may not all be single crystals and also have irregular external shapes that prevent their perfect alignment.

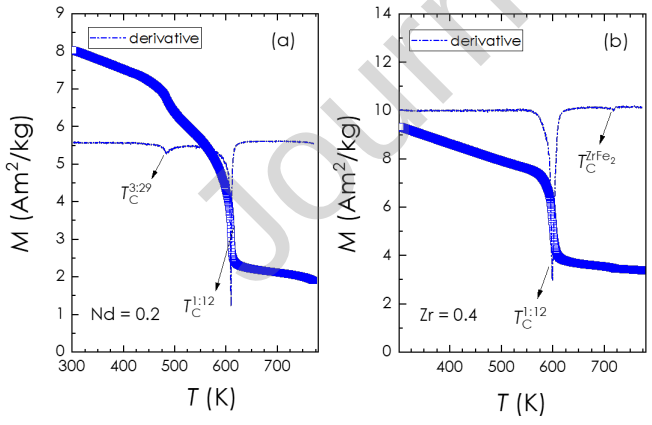

Figure 7: Typical thermomagnetic curves depicting T_C of different phases present in optimally heat-treated (a) $Sm_{0.8}Nd_{0.2}Fe_{11}V$ and (b) $Sm_{0.6}Zr_{0.4}Fe_{11}V$ alloys.

Values of T_C of 1:12 phase for $Sm_{1-x}Y_xFe_{11}V$ (Y=Nd, Zr) are summarized in Table 2. The optimally heat-treated $Sm_{1-x}Nd_xFe_{11}V$ alloys show that the T_C of 1:12 phase decreases from 625 to 593 K with increase of Nd from $x = 0$ to 0.4. In the case of $Sm_{1-x}Zr_xFe_{11}V$ alloys, T_C of 1:12 phase decreases from 625 to 583 K with the Zr-substitution from $x = 0$ to 0.6. Figure 7(a) and (b) shows typical thermomagnetic scans for heat-treated $Sm_{0.8}Nd_{0.2}Fe_{11}V$ and $Sm_{0.6}Zr_{0.4}Fe_{11}V$ alloys, respectively. The T_C is strongly determined by the transition metals M-M interaction. When Sm is substituted by Nd or Zr, the interatomic distances between the near neighbors of Fe atoms at the different sites are affected resulting in reduced total interaction causing a decrease in T_C.

The 1:12 is not the only magnetic phase present in these alloys, but there is also a small quantity of 3:29 phase in Nd-substituted alloy and $ZrFe_2$ in Zr-substituted alloy, which are also observed in XRD analysis. The T_C at 483 K in Fig. 7(a) corresponds to 3:29 phase and the T_C at 709 K in Fig. 7(b) corresponds to $ZrFe_2$ Laves phase. The T_C of 3:29 decreases from 483 to 473 K with increasing Nd from $x = 0.2$ to 0.4. The T_C of Laves phase decreases from 709 to 697 K with increasing Zr from $x = 0.4$ and 0.6. Brückner et al. [52] found that T_C of the Laves phase increases from 610 to 798 K as the Fe content increases from 66.7 to 72.3 at.%. Based on this dependency of the T_C on Fe concentration for $ZrFe_2$, we can say that Fe content in the Laves phase in the alloys studied in the current work is between 68.7 and 70.6 at.%.

4. Conclusions

Effects of Zr- and Nd-substitution for Sm on magnetic and structural properties in $SmFe_{11}V$ alloy were studied. For all the optimally heat-treated alloys, the main phase was found to be 1:12. As Zr content increased from $x = 0$ to 0.6, the $\mu_0 H_A$ decreased from 11 to 9 T and the T_C from 625 to 583 K while M_s increased from 115 to 138 $Am^2 kg^{-1}$. For high content of Zr ($x = 0.4$ and 0.6) Laves $ZrFe_2$ phase was formed. The volume fraction of $ZrFe_2$ and α-(Fe,V) increased with increasing Zr content. In the case of Nd-substitution, $\mu_0 H_A$, M_s and T_C decreased with increasing Nd content, the substitution of even small quantities of Sm by Nd promotes the formation of the 3:29 phase, which ruin the desired magnetic properties. The $Sm_{0.61}Zr_{0.40}Fe_{11.03}V_{0.96}$ alloy exhibits suitable intrinsic magnetic properties for permanent magnet applications, $\mu_0 M_s$=1.28 T, $\mu_0 H_A$=9.4 T and T_C=599 K. Also it contains only 4.6 at.% of rare-earth metal compared to the 7.7 at.% used in the $SmFe_{11}V$ alloy.

Acknowledgments

Authors would like to acknowledge the financial support from Fondo Nacional de Financiamiento para la Ciencia, la Tecnología y la Innovación Francisco José de Caldas - MinCiencias, Government of Principality of Asturias (Spain) under project MAGNES SV-PA-21-AYUD/2021/51822 and Novamag project under EU Horizon 2020 Programme [grant number 686056].

References

[1] S. Massari and M. Ruberti, "Rare earth elements as critical raw materials: Focus on international markets and future strategies," *Resources Policy*, vol. 38, no. 1, pp. 36–43, 2013.

[2] EU Commission, *Study on the review of the list of critical raw materials. Criticality Assessments*. European commission B-1049 Brussels: Luxembourg:Publications Office of the European Union, 2017.

[3] K. P. Skokov and O. Gutfleisch, "Heavy rare earth free, free rare earth and rare earth free magnets - Vision and reality," *Scr. Mater.*, vol. 154, pp. 289–294, 2018.

[4] A. Gabay and G. Hadjipanayis, "Recent developments in RFe_{12}-type compounds for permanent magnets," *Scr. Mater.*, vol. 154, pp. 284–288, sep 2018.

[5] F. De Boer, Y.-K. Huang, D. De Mooij, and K. Buschow, "Magnetic properties of a series of novel ternary intermetallics ($RFe_{10}V_2$)," *J. less-common Met.*, vol. 135, pp. 199–204, nov 1987.

[6] K. Buschow, "Magnetovolume effects in ternary compounds of the type $RFe_{12-x}T_x$ and $R_2Fe_{14}C$ (R=rare earth, T=Ti, V, Cr, Mo, W, Si)," *J. Less-Common Met.*, vol. 144, no. 1, pp. 65–69, 1988.

[7] R. Verhoef, F. De Boer, Z. Zhi-dong, and K. Buschow, "Moment reduction in $RFe_{12-x}T_x$ compounds (R=Gd, Y and T=Ti, Cr, V, Mo, W)," *J. Magn. Magn. Mater.*, vol. 75, pp. 319–322, dec 1988.

[8] B.-P. Hu, H.-S. Li, J. P. Gavigan, and J. M. D. Coey, "Intrinsic magnetic properties of the iron-rich $ThMn_{12}$-structure alloys $R(Fe_{11}Ti)$; R=Y, Nd, Sm, Gd, Tb, Dy, Ho, Er, Tm and Lu," *J. Phys. Condens. Matter*, vol. 1, pp. 755–770, jan 1989.

[9] B.-P. Hu, H.-S. Li, J. M. D. Coey, and J. P. Gavigan, "Magnetization of a $Dy(Fe_{11}Ti)$ single crystal," *Phys. Rev. B*, vol. 41, pp. 2221–2228, Feb 1990.

[10] M. Jurczyk, "Magnetic and crystallographic properties of $SmFe_{10-x}Co_xV_2$ compounds," *J. Less-Common Met.*, vol. 162, no. 1, pp. 149–154, 1990.

[11] L. Pareti, M. Solzi, G. Marusi, M. R. Ibarra, and P. A. Algarabel, "Effect of vanadium on the RE and Fe sublattice anisotropies in some $REFe_{12-x}V_x$(RE=Y,Er,Tb) tetragonal compounds," *J. Appl. Phys.*, vol. 70, no. 7, pp. 3753–3759, 1991.

[12] Y. Wang, G. Hadjipanayis, A. Kim, D. Sellmyer, and W. Yelon, "Structure and magnetic properties of $rfe10v_2n_x$ compounds," *J. Magn. Magn. Mater.*, vol. 104-107, pp. 1132–1134, 1992. Proceedings of the International Conference on Magnetism, Part II.

[13] X. C. Kou, T. S. Zhao, R. Grössinger, H. R. Kirchmayr, X. Li, and F. R. de Boer, "Magnetic phase transitions, magnetocrystalline anisotropy, and crystal-field interactions in the $RFe_{11}Ti$ series (where R=Y, Pr, Nd, Sm, Gd, Tb, Dy, Ho, Er, or Tm)," *Phys. Rev. B*, vol. 47, pp. 3231–3242, Feb 1993.

[14] H. Kim, Y. B. Kim, W. S. Park, C. S. Kim, T. K. Kim, and H.-M. Jin, "Anisotropy constants of $(Sm_{0.5}RE_{0.5})Fe_{11}Ti$ compounds (RE=rare earth)," *Journal of Korean Magnetics Society*, vol. 5, pp. 683–686, Oct 1995.

[15] A. Apostolov, R. Bezdushnyi, R. Damianova, N. Stanev, and I. Naumova, "The effect of absorbed hydrogen on the magnetic properties of $DyFe_{11}Ti$," *J. Magn. Magn. Mater.*, vol. 150, no. 3, pp. 393–398, 1995.

[16] O. Isnard, S. Miraglia, M. Guillot, and D. Fruchart, "Hydrogen effects on the magnetic properties of $RFe_{11}Ti$ compounds," *J. Alloys Compd.*, vol. 275-277, pp. 637–641, 1998.

[17] S. Nikitin, I. Tereshina, V. Verbetsky, and A. Salamova, "Transformations of magnetic phase diagram as a result of insertion of hydrogen and nitrogen atoms in crystalline lattice of $RFe_{11}Ti$ compounds," *J. Alloys Compd.*, vol. 316, no. 1, pp. 46–50, 2001.

[18] C. Piquer, O. Isnard, F. Grandjean, and G. L. Long, "Magnetic and Mössbauer spectral properties of $DyFe_{11}Ti$ and $DyFe_{11}TiH$," *J. Magn. Magn. Mater.*, vol. 265, no. 2, pp. 156–166, 2003.

[19] N. Tajabor, D. Fruchart, D. Gignoux, S. Miraglia, and L. Motevalizadeh, "Spin reorientation and first-order magnetisation process in $HoFe_{11-x}Co_xTi$ compounds," *J. Magn. Magn. Mater.*, vol. 314, no. 2, pp. 122–127, 2007.

[20] A. Schönhöbel, R. Madugundo, O. Y. Vekilova, O. Eriksson, H. Herper, J. Barandiarán, and G. Hadjipanayis, "Intrinsic magnetic properties of $SmFe_{12-x}V_x$ alloys with reduced V-concentration," *J. Alloys Compd.*, vol. 786, pp. 969–974, may 2019.

[21] L. V. B. Diop, M. D. Kuz'min, Y. Skourski, K. P. Skokov, I. A. Radulov, and O. Gutfleisch, "Determination of the crystal field parameters in $SmFe_{11}Ti$," *Phys. Rev. B*, vol. 102, p. 064423, Aug 2020.

[22] F. Pinkerton and D. Van Wingerden, "Magnetic hardening of $SmFe_{10}V_2$ by melt-spinning," *IEEE Trans. Magn.*, vol. 25, no. 5, pp. 3306–3308, 1989.

[23] Y. Wang, G. C. Hadjipanayis, A. Kim, N. C. Liu, and D. J. Sellmyer, "Magnetic and structural studies in Sm-Fe-Ti magnets," *J. Appl. Phys.*, vol. 67, pp. 4954–4956, may 1990.

[24] M. Okada, A. Kojima, K. Yamagishi, and M. Homma, "High coercivity in melt-spun $SmFe_{10}(Ti,M)_2$ ribbons (M=V/Cr/Mn/Mo)," *IEEE Trans. Magn.*, vol. 26, no. 5, p. 1376, 1990.

[25] L. Schultz, K. Schnitzke, and J. Wecker, "High coercivity in mechanically alloyed Sm-Fe-V magnets with a $ThMn_{12}$ crystal structure," *Appl. Phys. Lett.*, vol. 56, pp. 868–870, feb 1990.

[26] J. Ding and M. Rosenberg, "Magnetic hardening of melt-spun and crystallized Sm-Fe-V and Sm-(Fe,Co)-V alloys," *J. Less-Common Met.*, vol. 161, no. 2, pp. 369–374, 1990.

[27] D. Simon, H. Wuest, S. Hinderberger, T. Koehler, A. Marusczyk, S. Sawatzki, L. Diop, K. Skokov, F. Maccari, A. Senyshyn, H. Ehrenberg, and O. Gutfleisch, "Structural and magnetic properties of $Ce_{1-x}Sm_xFe_{11-y}Ti_1V_y$," *Acta Mater.*, vol. 172, pp. 131–138, 2019.

[28] A. Schönhöbel, R. Madugundo, J. Barandiarán, G. Hadjipanayis, D. Palanisamy, T. Schwarz, B. Gault, D. Raabe, K. Skokov, O. Gutfleisch, J. Fischbacher, and T. Schrefl, "Nanocrystalline Sm-based 1:12 magnets," *Acta Mater.*, vol. 200, pp. 652–658, 2020.

[29] A. Bolyachkin, H. Sepehri-Amin, M. Kambayashi, Y. Mori, T. Ohkubo, Y. Takahashi, T. Shima, and K. Hono, "Coercivity engineering in $Sm(Fe_{0.8}Co_{0.2})_{12}B_{0.5}$ thin films by Si grain boundary diffusion," *Acta Materialia*, vol. 227, p. 117716, 2022.

[30] A. Martin-Cid, D. Salazar, A. Schönhöbel, J. Garitaonandia, J. Barandiaran, and G. Hadjipanayis, "Magnetic properties and phase stability of tetragonal $Ce_{1-x}Sm_xFe_9Co_2Ti$ 1:12 phase for permanent magnets," *J. Alloys Compd.*, vol. 749, pp. 640–644, 2018.

[31] H. T. Kim, Y. B. Kim, C. S. Kim, T. K. Kim, and H. Jin, "Magnetocrystalline anisotropy of $(Sm_{0.5}RE_{0.5})Fe11Ti$ compounds (RE = Ce, Pr, Nd, Sm, Gd and Tb)," *J. Magn. Magn. Mater.*, vol. 152, no. 3, pp. 387–390, 1996.

[32] L. Zhao, R. Su, L. Wen, W. Li, X. Liu, Z. Zhang, R. Zhao, Y. Han, X. Zhang, and W. Li, "Intrinsically High Magnetic Performance in Core–Shell Structural (Sm,Y)Fe12-Based Permanent Magnets," *Advanced Materials*, vol. 34, no. 28, p. 2203503, 2022.

[33] D. Niarchos, M. Gjoka, A. M. Schönhöbel, A. Aubert, R. Madugundo, J. J. S. Garitaonandia, J. M. Barandiaran, and G. Hadjipanayis, "Intrinsic magnetic properties of $(Nd_{1-x}Sm_x)Fe_{11}Ti$," *J. Alloys Compd.*, vol. 864, p. 158097, 2021.

[34] P. Tozman, T. Fukazawa, D. Ogawa, H. Sepehri-Amin, A. Bolyachkin, T. Miyake, S. Hirosawa, K. Hono, and Y. Takahashi, "Peculiar behavior of v on the curie temperature and anisotropy field of smfe12-xvx compounds," *Acta Materialia*, vol. 232, p. 117928, 2022.

[35] D. Goll, R. Loeffler, R. Stein, U. Pflanz, S. Goeb, R. Karimi, and G. Schneider, "Temperature dependent magnetic properties and application potential of intermetallic $Fe_{11-x}Co_xTiCe$," *Phys. Status Solidi RRL*, vol. 8, no. 10, pp. 862–865, 2014.

[36] C. Zhou, F. E. Pinkerton, and J. F. Herbst, "Magnetic properties of $CeFe_{11-x}Co_xTi$ with $ThMn_{12}$ structure," *J. Appl. Phys.*, vol. 115, p. 17C716, may 2014.

[37] S. Suzuki, T. Kuno, K. Urushibata, K. Kobayashi, N. Sakuma, K. Washio, H. Kishimoto, A. Kato, and A. Manabe, "A $(Nd,Zr)(Fe,Co)_{11.5}Ti_{0.5}N_x$ compound as a permanent magnet material," *AIP Adv.*, vol. 4, p. 117131, nov 2014.

[38] S. Suzuki, T. Kuno, K. Urushibata, K. Kobayashi, N. Sakuma, K. Washio, M. Yano, A. Kato, and A. Manabe, "A new magnet material with $ThMn_{12}$ structure:," *J. Magn. Magn. Mater.*, vol. 401, pp. 259–268, mar 2016.

[39] P. Tozman, H. Sepehri-Amin, Y. K. Takahashi, S. Hirosawa, and K. Hono, "Intrinsic magnetic properties of $Sm(Fe_{1-x}Co_x)_{11}Ti$ and Zr-substituted $Sm_{1-y}Zr_y(Fe_{0.8}Co_{0.2})_{11.5}Ti_{0.5}$ compounds with $ThMn_{12}$ structure toward the development of permanent magnets," *Acta Mater.*, vol. 153, pp. 354–363, 2018.

[40] H. Du, J. Han, W. Zhang, C. Wang, W. Wang, S. Liu, H. Chen, X. Zhang, and Y. Yang, "Determination of the zirconium site in zirconium-substituted $Nd(Fe,Mo,Zr)_{12}$ compounds," *J. Magn. Magn. Mater.*, vol. 283, pp. 316–321, dec 2004.

[41] N. Sakuma, S. Suzuki, T. Kuno, K. Urushibata, K. Kobayashi, M. Yano, A. Kato, and A. Manabe, "Influence of Zr substitution on the stabilization of $ThMn_{12}$-type $(Nd_{1-\alpha}Zr_\alpha)(Fe_{0.75}Co_{0.25})_{11.25}Ti_{0.75}N_{1.2-1.4}$ ($\alpha = 0 -$

0.3) compounds," *AIP Adv.*, vol. 6, p. 056023, may 2016.
[42] S. Sakurada, A. Tsutai, and M. Sahashi, "A study on the formation of $ThMn_{12}$ and $NaZn_{13}$ structures in $RFe_{10}Si_2$," *J. Alloys Compd.*, vol. 187, pp. 67–71, aug 1992.
[43] A. M. Gabay and G. C. Hadjipanayis, "$ThMn_{12}$-type structure and uniaxial magnetic anisotropy in $ZrFe_{10}Si_2$ and $Zr_{1-x}Ce_xFe_{10}Si_2$ alloys," *J. Alloys Compd.*, vol. 657, pp. 133–137, 2016.
[44] A. M. Gabay, R. Cabassi, S. Fabbrici, F. Albertini, and G. C. Hadjipanayis, "Structure and permanent magnet properties of $Zr_{1-x}R_xFe_{10}Si_2$ alloys with R = Y, La, Ce, Pr and Sm," *J. Alloys Compd.*, vol. 683, pp. 271–275, 2016.
[45] J. Rodríguez-Carvajal, "Recent advances in magnetic structure determination by neutron powder diffraction," *Physica B Condens. Matter*, vol. 192, no. 1-2, pp. 55–69, 1993.
[46] H. M. Rietveld, "A profile refinement method for nuclear and magnetic structures," *J. Appl. Crystallogr.*, vol. 2, pp. 65–71, 1969.
[47] S. Sugimoto, T. Shimono, H. Nakamura, T. Kagotani, M. Okada, and M. Homma, "Phase Relation of Sm-Fe-V Alloys around the Compound $Sm_3(Fe,V)_{29}$," *Mater. Trans. JIM*, vol. 37, no. 3, pp. 494–498, 1996.
[48] R. L. Johannes, R. Haydock, and V. Heine, "Phase Stability in Transition-Metal Laves Phases," *Phys. Rev. Lett.*, vol. 36, pp. 372–376, feb 1976.
[49] N. N. Greenwood and A. Earnshaw, *Chemistry of the Elements*. Butterworth-Heinemann, second ed., 1997.
[50] M. Kataoka, T. Satoh, and E. Otsuki, "Structure and magnetic properties of $Sm_3(Fe,V)_{29}N_X$," *J. Appl. Phys.*, vol. 85, no. 8, pp. 4675–4677, 1999.
[51] J. Crangle, G. M. Goodman, and W. Sucksmith, "The magnetization of pure iron and nickel," *Proc. R. Soc. A: Math. Phys. Eng. Sci.*, vol. 321, no. 1547, pp. 477–491, 1971.
[52] W. Brückner, R. Perthel, K. Kleinstück, and G. E. R. Schulze, "Magnetic Properties of $ZrFe_2$ and $TiFe_2$ within Their Homogeneity Range," *Phys. Status Solidi B*, vol. 29, no. 1, pp. 211–216, 1968.
[53] T. Kuno, S. Suzuki, K. Urushibata, K. Kobayashi, N. Sakuma, M. Yano, A. Kato, and A. Manabe, "$(Sm,Zr)(Fe,Co)_{11.0-11.5}Ti_{1.0-0.5}$ compounds as new permanent magnet materials," *AIP Adv.*, vol. 6, no. 2, p. 025221, 2016.
[54] P. Tozman, Y. Takahashi, H. Sepehri-Amin, D. Ogawa, S. Hirosawa, and K. Hono, "The effect of Zr substitution on saturation magnetization in $(Sm_{1-x}Zr_x)(Fe_{0.8}Co_{0.2})_{12}$ compound with the $ThMn_{12}$ structure," *Acta Mater.*, vol. 178, pp. 114–121, 2019.
[55] S. Kobayashi, D. Ogawa, X. Xu, Y. Takahashi, A. Martin-Cid, K. Ishigami, Y. Kotani, M. Suzuki, T. Yoshioka, H. Tsuchiura, H. Sepehri-Amin, T. Ohkubo, K. Hono, S. Hirosawa, and T. Nakamura, "Multimodal analysis of Zr substitution effects on magnetic and crystallographic properties in $(Sm_{1-x}Zr_x)(Fe_{0.8}Co_{0.2})_{12}$ compounds with $ThMn_{12}$ structure," *Acta Materialia*, vol. 242, p. 118454, 2023.
[56] K.-D. Durst and H. Kronmüller, "Determination of intrinsic magnetic material parameters of $Nd_2Fe_{14}B$ from magnetic measurements of sintered $Nd_{15}Fe_{77}B_8$ magnets," *J. Magn. Magn. Mater.*, vol. 59, pp. 86–94, may 1986.
[57] S. K. Pal, K. P. Skokov, T. Groeb, S. Ener, and O. Gutfleisch, "Properties of magnetically semi-hard $(Fe_xCo_{1-x})3B$ compounds," *J. Alloys Compd.*, vol. 696, pp. 543–547, 2017.
[58] O. Gutfleisch, "Controlling the properties of high energy density permanent magnetic materials by different processing," *J. Phys. D: Appl. Phys.*, vol. 33, pp. 157–172, 2000.
[59] K. Buschow, "Chapter 4 Magnetism and processing of permanent magnet materials," in *Handbook of Magnetic Materials*, vol. 10, pp. 463–593, Elsevier Science, 1997.

CRediT author statement

A. M. Schönhöbel: Investigation, Formal analysis, Writing - Original Draft **R. Madugundo**: Investigation, Formal analysis, Writing - Review & Editing **C. Echevarria-Bonet**: Investigation, Writing - Review & Editing **L. E. Zamora**: Supervision **J. M. Barandiarán**: Supervision, Writing - Review & Editing, **G. C. Hadjipanayis**: Conceptualization.

Declaration of interests

☐The authors declare that they have no known competing financial interests or personal relationships that could have appeared to influence the work reported in this paper.

☒The authors declare the following financial interests/personal relationships which may be considered as potential competing interests:

A. M. Schonhobel reports financial support was provided by Colombia Ministry of Science Technology and Innovation. R. Madugundo, J.M. Barandiarán and Cristina Echevarria report financial support was provided by H2020 LEIT Advanced Materials. C. Echevarria-Bonet reports was provided by Government of Principality of Asturias.

Highlights

- We investigated the effects of substitution of Sm by RE element Nd and non RE element Zr on structure and magnetic properties in $Sm_{1-x}Y_xFe_{11}V$ (Y=Nd, Zr) alloys.
- The 1:12 phase is maintained throughout the Nd- and Zr- substitution.
- Substitution of Nd promotes the formation of α-(Fe,V) and 3:29 phase.
- As Zr content increases from x = 0 to 0.6, anisotropy field and Curie temperature decreases while saturation magnetization increases.
- The 1:12 phase with composition $Sm_{0.61}Zr_{0.40}Fe_{11.03}V_{0.96}$ exhibits optimum combination of magnetic properties of $\mu_0 M_s$ = 1.28 T, $\mu_0 H_A$ = 9.2 T and T_C = 599 K. It contains only 4.6 at. % of rare-earth metal compared to the 7.7 at. % used in the $SmFe_{11}V$ alloy.